

Spatial AI as Field-Programmable Reality Layers

A Geometric, Dynamical, and Information-Theoretic Framework for Environment-Centric Intelligence within the OCTA Research Program

OCTA Research

OCTA Research Technical Report

Version 1.1 – January 1, 2026

Abstract

We formalize *Spatial AI* as a field-theoretic paradigm in which physical spaces (rooms, buildings, vehicles, campuses) attain persistent identities and behaviors via dynamically maintained perception fields. Rather than treating intelligence as device- or cloud-centric, we model it as a property of an *environment*—a bounded region of space carrying a spatio-temporal field that encodes state, memory, and control.

Mathematically, a Spatial AI system is described by:

- a spatial domain (X, d) with boundary and interior nodes,
- a perception field $\phi : X \times \mathbb{R}_{\geq 0} \rightarrow \mathbb{R}^m$,
- a family of node-local oscillators $\{\theta_i\}_i$ enforcing phase coherence,
- a dynamical law $\dot{\phi} = F(\phi, u, \theta)$ whose attractor encodes the *identity* of the space,
- coherence functionals that distinguish normal operation from anomalies.

We develop continuous and discrete formulations, Lyapunov stability conditions, Bayesian and information-theoretic interpretations, and multi-scale decompositions. We then integrate *Perfect Attractor* geometry via an attractor center, inverse-square-like potentials, and warped metrics, yielding a geometric Laplacian that shapes room identity.

Within the broader *OCTA Research* program, Spatial AI is positioned as an environmental substrate for embodied AGI, interfacing with OCTA’s spiking, mesoscopic, and symbolic layers. TikZ diagrams depict room geometry, oscillator synchrony, attractor basins, and room composition; tables summarize symbols, metrics, and experimental protocols. The result is a comprehensive research framework for environment-centric intelligence suitable for rigorous simulation and eventual deployment in real-world structures.

Contents

1	Introduction	4
2	Spatial Substrate and Nodes	4
2.1	Geometric model of a space	4
2.2	Distributed nodes	5
2.3	TikZ diagram: a simple Spatial AI room	5
3	Perception Field	5

3.1	Field definition	5
3.2	Observation operators	6
3.3	Reconstruction as inverse problem	6
4	Room Identity as an Attractor	6
4.1	Dynamical law over fields	6
4.2	Identity attractor	7
4.3	Latent parameterization	7
4.4	TikZ: attractor basin	8
5	Coherence and Anomaly Measures	8
5.1	Spatial coherence	8
5.2	Temporal coherence	8
5.3	Combined anomaly score	9
5.4	Table: coherence metrics	9
6	Oscillator Network and Phase Coherence	9
6.1	Node-level oscillators	9
6.2	Global phase order parameter	9
6.3	Coupling to the perception field	10
6.4	TikZ: oscillator phases on the unit circle	10
7	Control and Behavior of the Space	10
7.1	Energy functional perspective	10
8	Composition of Spaces	11
8.1	Graph of rooms	11
8.2	Inter-space coupling	11
8.3	TikZ: composition of rooms	11
9	Learning the Identity of a Space	11
9.1	Data and objective	11
9.2	Attractor regularization	12
10	Stability, Robustness, and Guarantees	12
10.1	Lyapunov stability of identity	12
10.2	Robustness to node loss	13
11	Discrete and Implementable Formulation	13

11.1 Spatial discretization	13
11.2 Discrete oscillators	13
11.3 Table: discrete implementation variables	13
12 Bayesian Interpretation	14
12.1 Generative model	14
13 Information-Theoretic Coherence	14
14 Multi-Scale Spatial Decomposition	14
15 Safety Guarantees	15
16 Global Properties of Spatial AI Spaces	15
16.1 Emergent memory	15
16.2 Embodiment	15
17 Simulation and Evaluation	15
18 Perfect Attractor Geometry for Spatial AI	15
18.1 Attractor center and radial geometry	16
18.2 Warped metric and attractor Laplacian	16
18.3 Field dynamics with geometric potential	17
18.4 Geometric energy term	17
18.5 TikZ: 2D attractor potential in a room	17
18.6 Attractor geometry and identity stability	17
18.7 Discrete attractor geometry	18
18.8 Table: Perfect Attractor geometry → Spatial AI instantiation	18
19 OCTA Research Context and Roadmap	18
19.1 Spatial AI within the OCTA stack	18
19.2 Research phases (2026+ roadmap)	19
20 Conclusion	19
Appendix A: Symbol Summary	21
Appendix B: Perfect Attractor Geometric Parameters	22

1 Introduction

Traditional AI systems are device- or cloud-centric: models run on servers or embedded processors, operating on streams of sensor data. The physical environment is treated as a passive source of inputs and a passive sink for actions.

Spatial AI proposes a different viewpoint:

Intelligence is a property of a space, not only of a device.

Instead of attaching models to devices, we attach a *perception field* and a *dynamical identity* to bounded regions of space: rooms, buildings, vehicles, or outdoor sites. A room becomes an intelligent entity that:

- maintains a latent representation of itself over time,
- detects anomalies as decoherence of this latent representation,
- coordinates actions via distributed policies driven by a global field,
- composes with other rooms into building-scale intelligences.

This document develops a mathematical framework for Spatial AI as *Field-Programmable Reality Layers*. It integrates:

- partial differential equation (PDE) style field dynamics,
- Kuramoto-style oscillator networks,
- attractor theory and Lyapunov stability,
- Bayesian and information-theoretic perspectives,
- multi-scale spatial decompositions,
- safety constraints and implementable discretizations,
- Perfect Attractor geometry (attractor center, inverse-square potential, warped metric) as a structured prior over room identity.

Within the broader **OCTA Research** context, Spatial AI serves as the environmental layer that couples OCTA's internal cognitive engines to the physical world. Spatial fields become the medium where spiking dynamics, symbolic planning, and geometric attractors meet.

We use TikZ diagrams to visualize:

- a room with nodes and field structure,
- oscillator phase synchronization,
- attractor basins for spatial identity,
- composition of rooms into building-level intelligence,
- attractor potential geometry for a space,
- high-level OCTA–Spatial AI integration.

2 Spatial Substrate and Nodes

2.1 Geometric model of a space

Let (X, d) be a compact metric space representing a physical environment (e.g., a room, a floor, or a vehicle interior). For intuition, we may take $X \subset \mathbb{R}^3$ bounded and closed with the induced Euclidean metric, but the formalism does not depend critically on this.

We distinguish:

- the *interior* X° ,
- the *boundary* ∂X (walls, doors, windows, hull).

In OCTA-aligned deployments, X may also be a virtual or hybrid environment (e.g., digital twin) whose geometry is synchronized with physical sensors.

2.2 Distributed nodes

Let $N = \{1, \dots, n\}$ index the set of nodes (devices) deployed in X . Each node $i \in N$ has:

- a location $x_i \in X$,
- a local state $z_i(t) \in \mathbb{R}^{k_i}$,
- sensing channels $s_i(t) \in \mathbb{R}^{p_i}$,
- actuation channels $a_i(t) \in \mathbb{R}^{q_i}$.

We write the node configuration at time t as

$$\mathbf{z}(t) = (z_1(t), \dots, z_n(t)).$$

Nodes are connected by a time-varying graph:

$$G(t) = (N, E(t)), \quad E(t) \subseteq N \times N,$$

representing wireless, wired, or opportunistic connectivity.

2.3 TikZ diagram: a simple Spatial AI room



Figure 1: A Spatial AI room X with nodes $i \in N$ and a latent perception field (colored shading) spanning the entire space.

3 Perception Field

3.1 Field definition

A *perception field* is a function

$$\phi : X \times \mathbb{R}_{\geq 0} \rightarrow \mathbb{R}^m$$

assigning to each point $x \in X$ and time $t \geq 0$ a vector $\phi(x, t)$ representing latent environmental state (e.g., occupancy, motion, semantic labels, risk scores).

We assume $\phi(\cdot, t) \in L^2(X, \mathbb{R}^m)$ for each t , so that integrals and norms are well-defined.

3.2 Observation operators

Each node i provides noisy, partial observations of ϕ in a neighborhood of x_i .

Associate to each node i an observation operator

$$\mathcal{O}_i : L^2(X, \mathbb{R}^m) \rightarrow \mathbb{R}^{p_i},$$

and a measurement model

$$s_i(t) = \mathcal{O}_i\phi(\cdot, t) + \eta_i(t),$$

where $\eta_i(t)$ is noise (sensor and modeling).

A common structure is a localized kernel:

$$\mathcal{O}_i\phi(\cdot, t) = \int_X K_i(x, x_i)\phi(x, t) dx,$$

with K_i sharply peaked around x_i .

3.3 Reconstruction as inverse problem

Given $\{s_i(t)\}_{i \in N}$, the environment reconstructs $\phi(\cdot, t)$ by solving

$$\hat{\phi}(\cdot, t) \in \arg \min_{\psi \in L^2(X, \mathbb{R}^m)} \left\{ \sum_{i=1}^n \ell_i(\mathcal{O}_i\psi, s_i(t)) + \lambda \mathcal{R}(\psi) \right\},$$

where:

- ℓ_i is a local loss (e.g., squared error),
- \mathcal{R} is a regularizer enforcing smoothness and structure,
- $\lambda > 0$ is a regularization weight.

Unlike generic smoothing, \mathcal{R} will encode the *identity and typical dynamics* of the space (Section 4).

4 Room Identity as an Attractor

4.1 Dynamical law over fields

Let Φ denote the state space of fields, e.g. $\Phi = L^2(X, \mathbb{R}^m)$.

We model the evolution of ϕ via:

$$\frac{\partial \phi(x, t)}{\partial t} = F(x, \phi(\cdot, t), u(\cdot, t), \theta(t)), \quad x \in X, t \geq 0, \tag{1}$$

where:

- $u(\cdot, t)$ is an exogenous input field (human activity, weather),

- $\theta(t)$ are node oscillator phases (Section 6),
- F may depend on spatial derivatives of ϕ and non-local interactions.

A useful decomposition is:

$$F = \underbrace{D\Delta\phi}_{\text{diffusion/smoothing}} + \underbrace{H(\phi, u)}_{\text{habitual dynamics}} + \underbrace{C(\phi, \theta)}_{\text{coherence coupling}}, \quad (2)$$

where:

- D is a diffusion coefficient,
- Δ is the Laplace operator on X ,
- H encodes learned typical temporal patterns,
- C couples the field to oscillator phases, pulling toward phase-coherent configurations.

4.2 Identity attractor

Definition 1 (Spatial identity attractor). *A compact set $\mathcal{A} \subset \Phi$ is called an identity attractor of the spatial environment (X, F) if:*

- (i) \mathcal{A} is invariant under (1),
- (ii) \mathcal{A} is asymptotically stable: for an open neighborhood $U \supset \mathcal{A}$ and all $\phi_0 \in U$,

$$\lim_{t \rightarrow \infty} \text{dist}(\phi(\cdot, t; \phi_0), \mathcal{A}) = 0,$$

- (iii) \mathcal{A} has low effective dimension, e.g. approximated by a d -dimensional manifold with $d \ll \dim(\Phi)$.

4.3 Latent parameterization

We parameterize \mathcal{A} via a latent variable model:

$$\phi(x, t) \approx g(x, y(t)),$$

where:

- $y(t) \in \mathbb{R}^d$ is a low-dimensional latent coordinate,
- $g : X \times \mathbb{R}^d \rightarrow \mathbb{R}^m$ is a decoder mapping,
- the identity attractor corresponds to $\mathcal{Y} \subset \mathbb{R}^d$, with $\mathcal{A} = \{g(\cdot, y) : y \in \mathcal{Y}\}$.

Learning identity means learning:

- latent dynamics $\dot{y} = f(y, u)$,
- decoder g ,
- typical latent region \mathcal{Y} .

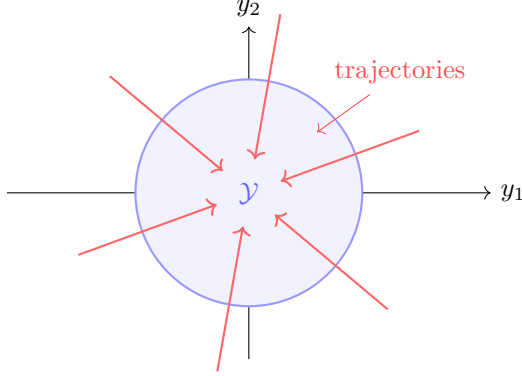


Figure 2: Latent space $y(t) \in \mathbb{R}^2$ with identity attractor region \mathcal{Y} as a basin. Trajectories converge toward \mathcal{Y} under normal operation.

4.4 TikZ: attractor basin

5 Coherence and Anomaly Measures

5.1 Spatial coherence

For a given field $\phi(\cdot, t)$, define spatial coherence:

$$C_{\text{space}}(t) = 1 - \frac{\int_X \|\phi(x, t) - \bar{\phi}(t)\|^2 dx}{\int_X \|\phi(x, t)\|^2 dx + \varepsilon}, \quad (3)$$

where

$$\bar{\phi}(t) = \frac{1}{\mu(X)} \int_X \phi(x, t) dx$$

is the spatial average and $\varepsilon > 0$ prevents division by zero.

$C_{\text{space}}(t) \in (0, 1]$; values near 1 indicate the field is spatially well-organized around a dominant pattern.

5.2 Temporal coherence

For a time window $T > 0$, define temporal coherence of $y(t)$:

$$C_{\text{time}}(t) = \exp \left(-\alpha \int_{t-T}^t \|\dot{y}(\tau) - \bar{y}_T(t)\|^2 d\tau \right),$$

where

$$\bar{y}_T(t) = \frac{1}{T} \int_{t-T}^t \dot{y}(\tau) d\tau,$$

and $\alpha > 0$ controls sensitivity.

High C_{time} indicates latent dynamics consistent with prior motion patterns.

5.3 Combined anomaly score

Define:

$$C(t) = C_{\text{space}}(t)^\beta C_{\text{time}}(t)^{1-\beta}, \quad \beta \in [0, 1],$$

and anomaly score

$$A(t) = 1 - C(t).$$

Sustained high $A(t)$ indicates structural deviation from identity.

5.4 Table: coherence metrics

Table 1: Core coherence metrics in Spatial AI.

Symbol	Name	Interpretation
$C_{\text{space}}(t)$	Spatial coherence	Organization of field over X
$C_{\text{time}}(t)$	Temporal coherence	Consistency of latent dynamics
$C(t)$	Total coherence	Joint spatial-temporal stability
$A(t)$	Anomaly score	Decoherence measure ($A = 1 - C$)
$r(t)$	Phase coherence (oscillators)	Synchrony of node phases
$C_{\text{info}}(t)$	Information coherence	Mutual information alignment

6 Oscillator Network and Phase Coherence

6.1 Node-level oscillators

Each node i maintains a phase $\theta_i(t) \in \mathbb{S}^1$ evolving as

$$\dot{\theta}_i = \omega_i + \sum_{j \in N} K_{ij} \sin(\theta_j - \theta_i) + \Gamma_i(\phi(\cdot, t), z_i(t)), \quad (4)$$

where:

- ω_i is the natural frequency,
- K_{ij} is the coupling coefficient (respecting edges of $G(t)$),
- Γ_i couples to field and local state.

6.2 Global phase order parameter

Define:

$$r(t)e^{j\psi(t)} = \frac{1}{n} \sum_{i=1}^n e^{j\theta_i(t)},$$

with $r(t) \in [0, 1]$ and $\psi(t) \in \mathbb{R}$.

- $r(t)$ measures phase coherence across nodes,
- $\psi(t)$ is the mean phase.

6.3 Coupling to the perception field

A simple coupling:

$$C(\phi, \theta)(x, t) = \kappa r(t)(\phi_*(x) - \phi(x, t)),$$

where:

- $\kappa > 0$ is coupling strength,
- ϕ_* is a learned “rest” field.

6.4 TikZ: oscillator phases on the unit circle

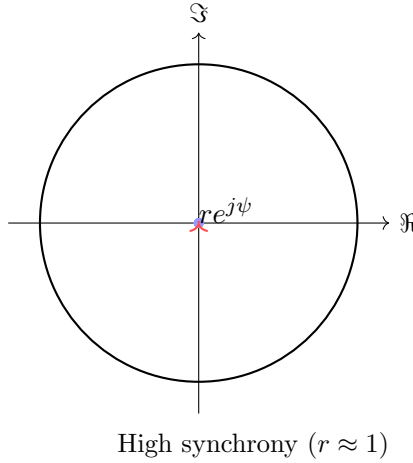


Figure 3: Oscillator phases θ_i on the complex unit circle with strong alignment (high r).

7 Control and Behavior of the Space

Each node implements a control policy:

$$a_i(t) = \pi_i(\phi(\cdot, t), s_i(t), z_i(t)),$$

mapping reconstructed field, local measurements, and internal state to actions (lighting, HVAC, doors, alarms, robots, displays, etc.).

Collectively, the environment realizes a distributed control system driven by the global field structure.

7.1 Energy functional perspective

Often, field dynamics can be written as a gradient flow:

$$\frac{\partial \phi}{\partial t} = -\frac{\delta \mathcal{E}}{\delta \phi},$$

with

$$\mathcal{E}(\phi) = \mathcal{E}_{\text{fit}}(\phi; s) + \mathcal{E}_{\text{habit}}(\phi) + \mathcal{E}_{\text{coh}}(\phi, \theta),$$

where:

- \mathcal{E}_{fit} penalizes mismatch with sensor data,
- $\mathcal{E}_{\text{habit}}$ encodes learned regularities,
- \mathcal{E}_{coh} encourages phase-aligned patterns.

Spatial AI seeks:

$$\min_{\phi, \theta} \mathcal{E}(\phi, \theta) \quad \text{subject to dynamics (1), (4).}$$

8 Composition of Spaces

8.1 Graph of rooms

Consider spaces $X^{(1)}, \dots, X^{(R)}$, each with field $\phi^{(r)}$ and identity attractor $\mathcal{A}^{(r)}$.

Let $\mathcal{G} = (\{1, \dots, R\}, \mathcal{E})$ be the adjacency graph of spaces (edges denote doors or shared boundaries).

We define an extended field

$$\Phi = (\phi^{(1)}, \dots, \phi^{(R)})$$

on $\bigsqcup_r X^{(r)}$ with coupling at shared boundaries.

8.2 Inter-space coupling

For $(r, s) \in \mathcal{E}$, define a boundary coupling:

$$J_{rs}(\phi^{(r)}, \phi^{(s)}) = \int_{\partial X^{(r)} \cap \partial X^{(s)}} \|\phi^{(r)}(x, t) - \phi^{(s)}(x, t)\|^2 d\sigma(x).$$

Building-level energy:

$$\mathcal{E}_{\text{building}}(\Phi, \theta) = \sum_{r=1}^R \mathcal{E}^{(r)}(\phi^{(r)}, \theta^{(r)}) + \sum_{(r,s) \in \mathcal{E}} \lambda_{rs} J_{rs}.$$

8.3 TikZ: composition of rooms

9 Learning the Identity of a Space

9.1 Data and objective

Let $\{s_i(t), a_i(t)\}_{i,t}$ be logs collected under normal operation.

We estimate:

$$\Theta = (F, g, f, \mathcal{E}_{\text{habit}}, \{\pi_i\}_i, \{\omega_i, K_{ij}\}_{i,j})$$

such that induced trajectories (ϕ, y, θ, a) best explain the data and exhibit a stable identity attractor.

We minimize:

$$\min_{\Theta} \mathbb{E}_{\text{data}} [L_{\text{fit}}(\Theta) + \lambda_{\text{attr}} L_{\text{attr}}(\Theta)],$$

where:

- L_{fit} measures prediction/reconstruction errors,
- L_{attr} measures attractor quality.

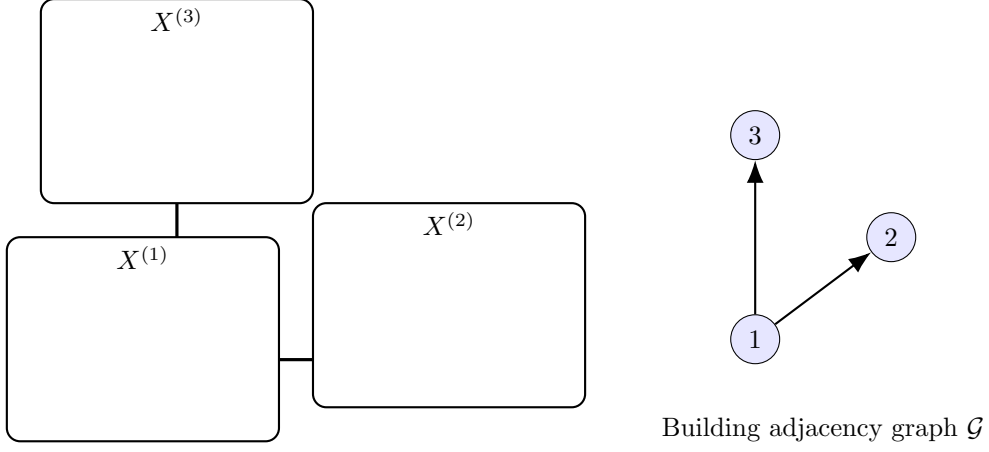


Figure 4: Multiple rooms $X^{(r)}$ with shared boundaries form a building. Their identity attractors are coupled, yielding building-scale behavior.

9.2 Attractor regularization

One practical regularizer enforces that $y(t)$ is largely low-dimensional. Let Σ_y be covariance of $y(t)$; then:

$$L_{\text{attr}}(\Theta) = \text{Tr}(\Sigma_y) - \sum_{k=1}^d \lambda_k(\Sigma_y),$$

with $\lambda_k(\Sigma_y)$ the ordered eigenvalues.

10 Stability, Robustness, and Guarantees

10.1 Lyapunov stability of identity

Theorem 1 (Lyapunov stability of spatial identity). *Suppose there exists a continuously differentiable functional $V : \Phi \rightarrow \mathbb{R}_{\geq 0}$ such that:*

- (i) $V(\phi) = 0$ iff $\phi \in \mathcal{A}$,
- (ii) $V(\phi) > 0$ otherwise,
- (iii) along trajectories of (1),

$$\frac{d}{dt} V(\phi(\cdot, t)) \leq -\gamma \|\phi(\cdot, t) - \Pi_{\mathcal{A}} \phi(\cdot, t)\|^2$$

for some $\gamma > 0$ and projection $\Pi_{\mathcal{A}}$.

Then \mathcal{A} is globally asymptotically stable.

Sketch. Standard Lyapunov arguments: V decreases along trajectories and can only reach zero on \mathcal{A} , forcing convergence. \square

10.2 Robustness to node loss

Definition 2 (Node robustness radius). *The identity attractor \mathcal{A} has robustness radius $\rho > 0$ if for all subsets $\tilde{N} \subseteq N$ with $|\tilde{N}| \geq (1 - \rho)|N|$, the attractor estimated from \tilde{N} remains within ϵ of \mathcal{A} in Φ .*

Under restricted injectivity conditions on $\{\mathcal{O}_i\}$ analogous to compressed sensing RIP, such a $\rho > 0$ exists, meaning the space retains identity even under partial node failure.

11 Discrete and Implementable Formulation

11.1 Spatial discretization

Partition X into M voxels $\{x_1, \dots, x_M\}$. Then

$$\phi(x, t) \rightsquigarrow \Phi(t) \in \mathbb{R}^{M \times m}.$$

Let $L \in \mathbb{R}^{M \times M}$ be a discrete Laplacian. Dynamics:

$$\dot{\Phi} = DL\Phi + H(\Phi, u) + C(\Phi, \theta).$$

11.2 Discrete oscillators

Nodes follow:

$$\dot{\theta}_i = \omega_i + \sum_j K_{ij} \sin(\theta_j - \theta_i) + \Gamma_i(\Phi, z_i).$$

Synchrony index:

$$r = \frac{1}{n} \left| \sum_i e^{j\theta_i} \right|.$$

11.3 Table: discrete implementation variables

Table 2: Key discrete variables for implementation.

Symbol	Type	Meaning
$\Phi \in \mathbb{R}^{M \times m}$	Matrix	Discretized field over M cells
$L \in \mathbb{R}^{M \times M}$	Matrix	Discrete Laplacian
$\theta \in \mathbb{R}^n$	Vector	Node phases
$K \in \mathbb{R}^{n \times n}$	Matrix	Phase coupling weights
$z_i \in \mathbb{R}^{k_i}$	Vector	Node internal state
$s_i \in \mathbb{R}^{p_i}$	Vector	Node measurements
$a_i \in \mathbb{R}^{q_i}$	Vector	Node actions

12 Bayesian Interpretation

12.1 Generative model

Treat ϕ as a latent random field:

$$\begin{aligned}\phi(\cdot, t) &\sim p(\phi \mid \phi(\cdot, t - \Delta t)), \\ s_i(t) &\sim p(s_i \mid \mathcal{O}_i \phi(\cdot, t)).\end{aligned}$$

Posterior:

$$p(\phi \mid s_{1:n}(0 : t)).$$

The identity attractor corresponds to *typical high-probability trajectories* under this posterior.

Conceptually:

$$\text{identity} \approx \text{Bayesian prior} + \text{stable posterior orbit}.$$

13 Information-Theoretic Coherence

Define a normalized field magnitude distribution $p_\phi(x, t)$ and entropy:

$$H(\phi(t)) = - \int_X p_\phi(x, t) \log p_\phi(x, t) dx.$$

Mutual information between field and sensors:

$$I(\phi; s_{1:n}) = H(\phi) - H(\phi \mid s_{1:n}).$$

Define information coherence:

$$C_{\text{info}}(t) = \frac{I(\phi; s_{1:n})}{H(\phi)}.$$

High C_{info} means sensors strongly constrain the field.

14 Multi-Scale Spatial Decomposition

Spaces have structure at multiple scales. Introduce basis $\{w_k(x)\}$, e.g. wavelets, such that:

$$\phi(x, t) = \sum_k \alpha_k(t) w_k(x).$$

Identity corresponds to a stable low-dimensional subset in α -space.

Large-scale anomalies manifest as macro-mode changes; local anomalies as high-frequency decoherence.

15 Safety Guarantees

We require bounded actions:

$$\|a_i(t)\| \leq B, \quad \left\| \frac{da_i}{dt} \right\| \leq L.$$

We also define a safety energy $\mathcal{E}_{\text{safety}}(\phi, a)$ with:

$$\frac{d}{dt} \mathcal{E}_{\text{safety}}(\phi, a) \leq 0$$

under anomaly-handling policies.

This yields monotonic approach to safe configurations.

16 Global Properties of Spatial AI Spaces

16.1 Emergent memory

If $\phi(\cdot, t)$ remains in a neighborhood of \mathcal{A} , then similar states at times t_1, t_2 correspond to similar field structures:

$$\phi(\cdot, t_1) \approx \phi(\cdot, t_2).$$

The environment *remembers* typical patterns in its attractor.

16.2 Embodiment

Intelligence is no longer confined to a device; it is instantiated as a property of space itself via ϕ , F , and \mathcal{A} .

17 Simulation and Evaluation

To evaluate Spatial AI, we consider:

- synthetic rooms with controllable human trajectories,
- controlled anomalies (intrusions, failures, unusual behavior),
- stochastic field perturbations,
- node dropout and communication failures,
- adversarial input noise and spoofing.

Metrics:

$$C(t), A(t), r(t), C_{\text{info}}(t), \text{dist}(\phi, \mathcal{A}), \text{time-to-recover}.$$

18 Perfect Attractor Geometry for Spatial AI

Spatial AI so far has been formulated on a generic metric space (X, d) with a standard Laplacian Δ (or its discrete counterpart L). We now enrich this with geometric structure inspired by the *Perfect Attractor* paradigm: a distinguished attractor center, an inverse-square-like potential, and a warped metric that encodes “where the room wants to stabilize.”

Table 3: Example evaluation metrics in simulated environments.

Metric	Type	Target behavior	Interpretation
$C(t)$	Scalar	High in nominal	Global coherence
$A(t)$	Scalar	Low in nominal	Anomaly magnitude
$r(t)$	Scalar	High in nominal	Phase synchrony
$C_{\text{info}}(t)$	Scalar	High in nominal	Sensor informativeness
TTR	Time	Small	Time-to-recover after anomaly

18.1 Attractor center and radial geometry

Let $x_0 \in X$ denote a distinguished *attractor center* for the space (e.g., a geometric or functional center of the room: a hub corridor, central column, or semantic focal point).

Define the radial distance:

$$r(x) := d(x, x_0).$$

We introduce a geometric weighting function $w_A : X \rightarrow (0, \infty)$ and a potential $V_A : X \rightarrow \mathbb{R}$ of inverse-square flavor:

$$\begin{aligned} w_A(x) &= \frac{1}{1 + (r(x)/R_0)^2}, \\ V_A(x) &= \frac{\alpha}{r(x)^2 + \epsilon}, \end{aligned}$$

where:

- $R_0 > 0$ sets a characteristic length scale of the attractor,
- $\alpha > 0$ controls attractor strength,
- $\epsilon > 0$ avoids singularity at $r = 0$.

Intuitively:

- $w_A(x)$ modulates how much spatial variation is allowed: near the attractor center, changes are “stiffer”;
- $V_A(x)$ pulls the field and latent state toward the center, acting as an attractor potential for room identity.

18.2 Warped metric and attractor Laplacian

We define an *attractor-weighted metric* d_A by

$$ds_A^2 = w_A(x) ds^2,$$

where ds^2 is the line element corresponding to the original metric d (for $X \subset \mathbb{R}^3$, this is the usual Euclidean metric).

The associated attractor Laplacian Δ_A on smooth functions $\varphi : X \rightarrow \mathbb{R}^m$ is

$$\Delta_A \varphi(x) = \nabla \cdot (w_A(x) \nabla \varphi(x)).$$

Compared to the standard Laplacian Δ , Δ_A :

- amplifies smoothing where w_A is large (near attractor center),
- allows more variation where w_A is small (far from center),
- encodes a geometric preference for coherent structure around x_0 .

18.3 Field dynamics with geometric potential

We refine the field dynamics (2) to:

$$\frac{\partial \phi}{\partial t} = D\Delta_A \phi - \nabla V_A(x) \cdot \nabla \phi + H(\phi, u) + C(\phi, \theta), \quad (5)$$

where the geometric terms

$$D\Delta_A \phi \quad \text{and} \quad -\nabla V_A(x) \cdot \nabla \phi$$

jointly enforce that:

- the field is smoothly organized with respect to the attractor geometry,
- gradients are discouraged from pointing “against” the attractor except where strongly supported by data.

This aligns the identity attractor \mathcal{A} with the geometric potential landscape of the room: the room identity becomes a *geometric attractor* as well as a dynamical one.

18.4 Geometric energy term

We augment the energy functional with a geometric term $\mathcal{E}_{\text{geom}}$:

$$\mathcal{E}(\phi, \theta) = \mathcal{E}_{\text{fit}}(\phi; s) + \mathcal{E}_{\text{habit}}(\phi) + \mathcal{E}_{\text{coh}}(\phi, \theta) + \mathcal{E}_{\text{geom}}(\phi),$$

with

$$\mathcal{E}_{\text{geom}}(\phi) = \int_X V_A(x) \|\phi(x, t) - \phi_{\star}(x)\|^2 dx,$$

where ϕ_{\star} is the learned rest field.

Higher $V_A(x)$ means deviations from $\phi_{\star}(x)$ are more costly. Thus:

- near x_0 the field is strongly pinned to its typical identity,
- far from x_0 the room can express more variation and adaptivity.

18.5 TikZ: 2D attractor potential in a room

18.6 Attractor geometry and identity stability

The geometric term $\mathcal{E}_{\text{geom}}$ contributes to Lyapunov stability. Consider a Lyapunov functional

$$V(\phi) = \mathcal{E}_{\text{fit}}(\phi) + \mathcal{E}_{\text{habit}}(\phi) + \mathcal{E}_{\text{geom}}(\phi).$$

If:

- $V(\phi) \geq 0$ and $V(\phi) = 0$ only on \mathcal{A} ,
- and $\frac{d}{dt}V(\phi(\cdot, t)) \leq 0$ under (5),

then the attractor geometry reinforces convergence to \mathcal{A} . Moreover, since $V_A(x)$ is stronger near x_0 , the identity is *most rigid* in a geometrically central region and more flexible toward the periphery, matching how many real environments behave.

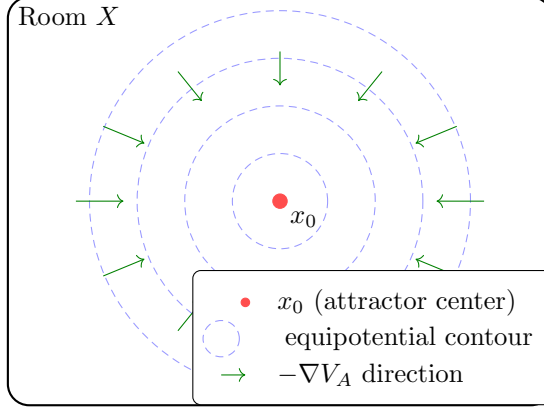


Figure 5: Attractor potential geometry in a room: x_0 is the center, dashed circles are level sets of $V_A(x)$, and arrows indicate the direction of steepest descent of the potential. Field dynamics and room identity are shaped by this attractor geometry.

18.7 Discrete attractor geometry

In the discretized setting with cells x_1, \dots, x_M , we define:

$$r_j = d(x_j, x_0), \quad w_{A,j} = \frac{1}{1 + (r_j/R_0)^2}, \quad V_{A,j} = \frac{\alpha}{r_j^2 + \epsilon},$$

and form diagonal matrices

$$W_A = \text{diag}(w_{A,1}, \dots, w_{A,M}), \quad V_A^{\text{diag}} = \text{diag}(V_{A,1}, \dots, V_{A,M}).$$

The discrete attractor Laplacian becomes

$$L_A = W_A L,$$

and the discrete geometric energy term is:

$$\mathcal{E}_{\text{geom}}(\Phi) = \sum_{j=1}^M V_{A,j} \|\Phi_{j,:} - \phi_{\star}(x_j)\|^2,$$

where $\Phi_{j,:}$ is the m -dimensional row vector at cell j .

18.8 Table: Perfect Attractor geometry → Spatial AI instantiation

19 OCTA Research Context and Roadmap

19.1 Spatial AI within the OCTA stack

Within OCTA Research, Spatial AI is conceived as the *environmental layer* interfacing:

- upward to cognitive engines (spiking networks, symbolic planners, generative models),
- downward to physical sensors and actuators,
- laterally to other Spatial AI spaces via P3P and mesh protocols.

Table 4: Mapping Perfect Attractor geometric ideas into Spatial AI.

Perfect Attractor concept	Spatial AI instantiation	Effect
Central attractor point	$x_0 \in X$	Reference for radial structure
Inverse-square field	$V_A(x) = \alpha/(r^2 + \epsilon)$	Pulls identity toward geometric center
Radial shells / levels	Level sets of V_A or w_A	Concentric zones of stiffness/flexibility
Attractor metric	$ds_A^2 = w_A(x)ds^2$	Warps diffusion and smoothing across space
Attractor basin	Identity attractor \mathcal{A}	Stable set of room field configurations
Geometry-driven flow	$\Delta_A, \nabla V_A$	Guides field evolution along structured paths

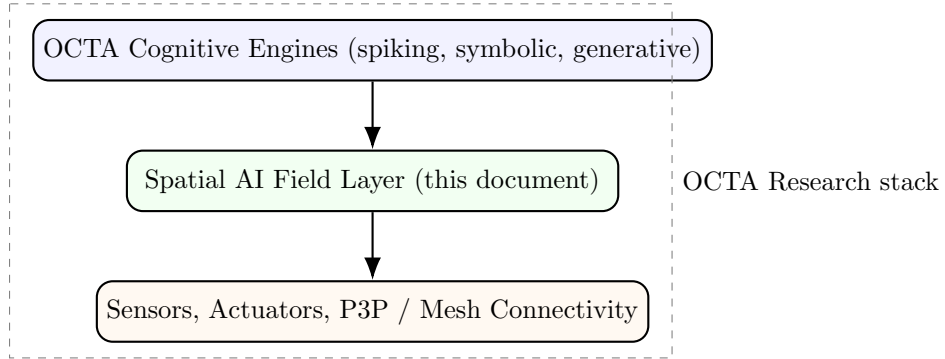


Figure 6: Positioning of Spatial AI in the OCTA Research stack.

19.2 Research phases (2026+ roadmap)

Table 5: High-level OCTA Research roadmap for Spatial AI.

Phase	Year	Focus
I	2026	Formalization, toy simulations, stability proofs for single rooms.
II	2026–2027	Multi-room buildings, mesh connectivity, anomaly benchmarks.
III	2027+	Integration with full OCTA cognitive stack and real-world pilot deployments.

20 Conclusion

Spatial AI reframes intelligence as a field-structured property of physical environments. Instead of hosting models on isolated devices, we attach a perception field, an identity attractor, a coherence structure, and now a Perfect Attractor geometry to spaces themselves.

Key conceptual shifts:

- Intelligence is *space-centric*, not merely device-centric.
- Normality is defined by *coherent field configurations*, not independent thresholds on raw signals.

- Anomalies are detected as *decoherence* or departures from a learned attractor.
- Control emerges from *distributed policies* conditioned on the global field.
- Geometry acts as a *prior* on where and how identity stabilizes inside a space.
- Within OCTA Research, Spatial AI is the environmental substrate through which AGI-like systems touch and shape the world.

This mathematical and systems framework provides a foundation for field-programmable, identity-bearing spaces that sense, remember, and act as coherent agents in their own right, with their dynamics shaped by physically meaningful attractor geometry.

Appendix A: Symbol Summary

Table 6: Summary of key symbols in Spatial AI.

Symbol	Domain	Meaning
X	Metric space	Physical environment (room)
d	Metric	Distance on X
N	Finite set	Indices of nodes
x_i	X	Location of node i
$\phi(x, t)$	\mathbb{R}^m	Perception field at point x
Φ	Function space	State space of fields
$z_i(t)$	\mathbb{R}^{k_i}	Node internal state
$s_i(t)$	\mathbb{R}^{p_i}	Node measurements
$a_i(t)$	\mathbb{R}^{q_i}	Node actions
\mathcal{O}_i	Operator	Observation operator for node i
$G(t)$	Graph	Node connectivity
F	Operator	Field dynamics law
$u(\cdot, t)$	Field	Exogenous input
$\theta_i(t)$	\mathbb{S}^1	Phase of node i
\mathcal{A}	Subset of Φ	Identity attractor
$y(t)$	\mathbb{R}^d	Latent representation
g	Decoder	Map from latent space to field
$C(t)$	$[0, 1]$	Coherence metric
$A(t)$	$[0, 1]$	Anomaly score ($1 - C$)
$r(t)$	$[0, 1]$	Phase coherence index
\mathcal{E}	Functional	Energy of field configuration
L	Matrix	Discrete Laplacian
K_{ij}	Scalar	Phase coupling
ω_i	Scalar	Natural frequency of node i

Appendix B: Perfect Attractor Geometric Parameters

Table 7: Geometric parameters introduced by the Perfect Attractor structure.

Symbol	Domain	Meaning
x_0	X	Attractor center of the room
$r(x)$	$\mathbb{R}_{\geq 0}$	Radial distance $d(x, x_0)$
R_0	$\mathbb{R}_{>0}$	Characteristic attractor radius
α	$\mathbb{R}_{>0}$	Strength of attractor potential
ϵ	$\mathbb{R}_{>0}$	Small constant to avoid singularity
$w_A(x)$	$(0, \infty)$	Attractor weight on metric / diffusion
$V_A(x)$	\mathbb{R}	Attractor potential energy at x
Δ_A	Operator	Attractor-weighted Laplacian
W_A	Diagonal matrix	Discrete attractor weights per cell
$V_{A,j}$	\mathbb{R}	Discrete potential at cell x_j
L_A	Matrix	Attractor-weighted discrete Laplacian
$\mathcal{E}_{\text{geom}}$	Functional	Geometric energy regularizer